

2 Fundamentals of Water Electrolysis

Pierre Millet

2.1 Thermodynamics of the Water Splitting Reaction

2.1.1 Thermodynamic Functions of State

Liquid water can be dissociated into its elemental components (molecular hydrogen and oxygen) according to:



In standard conditions of temperature and pressure ($T^\circ = 298 \text{ K}$, $P^\circ = 1 \text{ bar}$), water is liquid and H_2 and O_2 are gaseous. Enthalpy, entropy and free (Gibbs) energy standard changes for reaction (2.1) are, respectively [1]:

$$\Delta H_{\text{d}}^\circ(\text{H}_2\text{O}(\text{l})) = +285.840 \text{ kJ mol}^{-1}$$

$$\Delta S_{\text{d}}^\circ(\text{H}_2\text{O}(\text{l})) = +163.15 \text{ J mol}^{-1} \text{ K}^{-1}$$

$$\Delta G_{\text{d}}^\circ(\text{H}_2\text{O}(\text{l})) = \Delta H_{\text{d}}^\circ(\text{H}_2\text{O}(\text{l})) - T \cdot \Delta S_{\text{d}}^\circ(\text{H}_2\text{O}(\text{l})) = +237.22 \text{ kJ mol}^{-1}$$

In spite of a favourable entropic contribution due to the formation of 1.5 mole of gaseous species, the enthalpy change is strongly endothermic and, as a result, the Gibbs free energy change is positive and the reaction is non-spontaneous.

Water vapour can also be dissociated into gaseous hydrogen and oxygen according to:



Enthalpy, entropy and free (Gibbs) energy standard changes for reaction (2.2) are respectively [2]:

$$\Delta H_{\text{d}}^\circ(\text{H}_2\text{O}(\text{vap})) = +241.80 \text{ kJ mol}^{-1}$$

$$\Delta S_{\text{d}}^\circ(\text{H}_2\text{O}(\text{vap})) = +44.10 \text{ J mol}^{-1} \text{ K}^{-1}$$

$$\Delta G_{\text{d}}^\circ(\text{H}_2\text{O}(\text{l})) = \Delta H_{\text{d}}^\circ(\text{H}_2\text{O}(\text{l})) - T \cdot \Delta S_{\text{d}}^\circ(\text{H}_2\text{O}(\text{l})) = +228.66 \text{ kJ mol}^{-1}$$

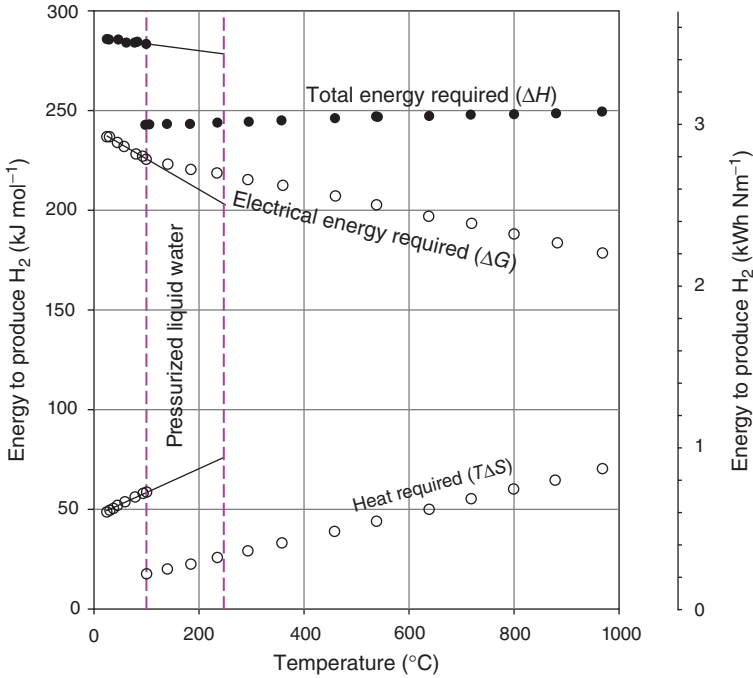


Figure 2.1 $\Delta G(T)$, $\Delta H(T)$ and $T\Delta S(T)$ of the water splitting reaction at $P = 1$ bar. (—) data for pressurized liquid water up to 250 °C.

$\Delta H_d^\circ(\text{H}_2\text{O}(\text{l})) - \Delta H_d^\circ(\text{H}_2\text{O}(\text{vap})) = +44.04 \text{ kJ mol}^{-1}$ is the difference of enthalpy change due to water vapourization (reaction 2.3) in standard conditions:



$\Delta S_d^\circ(\text{H}_2\text{O}(\text{l})) - \Delta S_d^\circ(\text{H}_2\text{O}(\text{vap})) = +119.05 \text{ J mol}^{-1} \text{ K}^{-1}$ is the difference of entropy change due to water vapourization.

State function changes with temperature ($\Delta G(T)$, $\Delta H(T)$ and $T \cdot \Delta S(T)$) for reaction (2.1) at 1 bar are plotted in Figure 2.1. The total energy ΔH required to split 1 mole of water is almost constant over the entire temperature range of practical interest. The entropy change ΔS is also approximately constant and positive and the entropic contribution $T \cdot \Delta S$ increases with temperature. The Gibbs free energy change $\Delta G = \Delta H - T \cdot \Delta S$ is positive but decreases when increasing the operating temperature. ΔG becomes negative at high temperatures ($>2500 \text{ K}$). Few if any materials can sustain such conditions and, therefore, the direct thermodissociation of water is not considered for practical applications. Discontinuities on $\Delta H(100^\circ\text{C}, 1\text{b})$ and $T \cdot \Delta S(100^\circ\text{C}, 1\text{b})$ observed at 100°C are due to water vapourization. The magnitude of the enthalpy discontinuity is equal to the standard enthalpy of water vapourization ($\approx +45 \text{ kJ mol}^{-1}$) and equal to the decrease of the entropic contribution. The slope difference of $T \cdot \Delta S(T)$, before and after

100 °C, reflects the entropy change after water vapourization. In Figure 2.1, solid lines between 100 and 250 °C show the situation for the electrolysis of liquid water above 100 °C (electrolysis of pressurized liquid water).

In conclusion, a higher operating temperature facilitates the dissociation of water by decreasing the electrolysis voltage. At room temperature, 15% of the total energy required for electrolysis of water comes from heat and 85% from electricity. At 1000 °C, one-third comes from heat and two-third from electricity. This is why high-temperature water electrolysis is interesting when heat is available: electrolysis requires less electricity (which is more expensive than heat).

2.1.2

Selection Criteria for Operating Temperature

According to Figure 2.1, water electrolysis can be performed at different operating temperatures. The question is, What is the best temperature? At any operating temperature T , $\Delta H(T)$ is the total amount of energy that is required to split 1 mole of water, $\Delta G(T)$ is the amount of electrical work needed and $T \cdot \Delta S(T)$ is the heat demand. The following relationship is satisfied:

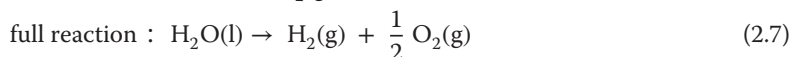
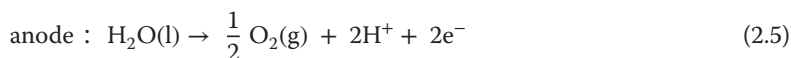
$$\Delta H(T, 1) = \Delta G(T, 1) + T \cdot \Delta S(T, 1) \quad (2.4)$$

ΔH (the total amount of energy required to split 1 mole of water) is temperature-independent but the higher the operating temperature, the less electricity is required and the more heat can be used. A first criterion that can be used to select the operating temperature is the cost ratio of the kilowatt hours of electricity to the kilowatt hours of heat, which is usually close to 3–5. Indeed, when heat is used in the industry to produce electricity, the overall efficiency is close to the Carnot efficiency, which is $\approx 30\%$ in conventional systems. In Europe, the cost of industrial heat is $\approx 10\text{--}15 \text{ € MWh}^{-1}$ and the cost of industrial electricity is $\approx 50\text{--}100 \text{ € MWh}^{-1}$. Therefore, operational expenses (opexs) are less for high-temperature electrolysis than for low-temperature electrolysis. As a result, the electricity consumption is higher at low temperature ($4\text{--}6 \text{ kWh Nm}^{-3} \text{ H}_2$ for PEM/alkaline technology (polymer electrolyte membrane = PEM)) than at high temperature ($3.4 \text{ kWh Nm}^{-3} \text{ H}_2$ for solid oxide water electrolysis (SOWE)). Another advantage of high-temperature water electrolysis is that it can potentially be used to value industrial heat wastes ($200\text{--}300 \text{ °C}$ is sufficient to vapourize liquid water, the heat of vapourization being a significant energy term in the water splitting reaction). A second criterion (the maturity of the technology) is less favourable to high-temperature technology, which is facing several problems (mostly from material science viewpoints, differential dilatation and interdiffusion phenomena being the source of high and still unacceptable degradation rates) and limitations (e.g. pressurized high-temperature water electrolysis cannot be envisioned in the near future due to severe leak management problems). A more detailed discussion on these issues is provided in the next sections.

2.1.3

Electrochemical Water Splitting

Thermodynamics tells us that the water splitting reaction is a non-spontaneous transformation. However, it can be driven externally by providing energy to the system, for example, electricity. This is a so-called endergonic transformation and the device used for the process is an electrolyser. An electrolyser contains at least one electrolysis cell. An electrolysis has two electrodes (electronic conductor) placed face to face and separated by a thin layer of ionic conductor (the electrolyte). In water electrolysis cells, electrical work is provided to the cell to split water molecules into gaseous hydrogen and oxygen. Half-cell reactions (and associated mechanisms) depend on electrolyte pH. In acidic media, water splitting occurs according to:



Equation 2.5 is the oxygen evolution reaction (OER) and Equation 2.6 is the hydrogen evolution reaction (HER). In aqueous media, protons formed at the oxygen-evolving anode are solvated to form hydronium ions H_3O^+ . Because of the electric field set across the cell, H_3O^+ species migrate through the electrolyte layer down to the cathode where they are reduced into molecular hydrogen while solvating water molecules are released. In terms of mass balance, there is a net consumption of water molecules at the anode and production of gases at each of the two-electrode/electrolyte interfaces. From the energy viewpoint and according to the first principle of thermodynamics, the amount of electricity (nFE) required at equilibrium to split 1 mole of water according to Equation 2.7 is equal to the Gibbs free energy change (ΔG_d) of the water dissociation reaction:

$$\Delta G_d - nFE = 0 \quad \text{where } \Delta G_d > 0 \quad (2.8)$$

where $n = 2$ is the number of electrons exchanged during the electrochemical splitting of one water molecule; $F \approx 96485 \text{ C mol}^{-1}$ is the Faraday constant, that is, the electric charge of 1 mole of electrons; and E (in volts) is the free energy electrolysis voltage associated with reaction (2.7). ΔG_d (in J mol^{-1}) is the free energy change associated with reaction (2.7).

For transformations occurring at constant temperature T and pressure P , one can write:

$$\Delta G_d(T, P) = \Delta H_d(T, P) - T \Delta S_d(T, P) > 0 \quad (2.9)$$

$\Delta H_d(T, P)$, $\Delta S_d(T, P)$ and $\Delta G_d(T, P)$ are, respectively, the enthalpy change (in J mol^{-1}), the entropy change (in $\text{J mol}^{-1} \text{K}^{-1}$) and the Gibbs free energy change (in J mol^{-1}) of reaction (2.7) occurring at T and P . As shown with Figure 2.1, ΔG_d (J mol^{-1}) of electricity and $T \cdot \Delta S_d$ (J mol^{-1}) of heat are required to split 1 mole of water.

Two different thermodynamic voltages are usually used to characterize water electrolysis.

The free energy electrolysis voltage E in volts is defined as:

$$E(T, P) = \frac{\Delta G_d(T, P)}{n F} \quad (2.10)$$

The enthalpy or thermo-neutral voltage V in volts is defined as:

$$V(T, P) = \frac{\Delta H(T, P)}{n F} \quad (2.11)$$

Different situations occur depending on the value of $U(T, P)$, the cell voltage applied to the electrolysis cell. For $U(T, P) < E(T, P)$, electrolysis does not start. For $E(T, P) < U(T, P) < V(T, P)$, there is enough electricity to initiate the process but not enough to maintain isothermicity. Because an electrolysis cell is an open system, the cell tends to take the heat required by the process from the surroundings. If not, the internal temperature should decrease. In fact, current starts to flow for $U(T, P) > E(T, P)$ and heat is produced internally by different irreversibility sources. Also, there is no practical interest to perform electrolysis in this voltage range because current density is so low that capital expenses (capexs) would be by far too expensive. Finally, for $U(T, P) > V(T, P)$, the current density increases and increasing amounts of heat are produced.

Reference electrolysis voltages are usually calculated in standard conditions of temperature ($T^\circ = 298 \text{ K}$) and pressure ($P^\circ = 1 \text{ bar}$). Water is liquid, H_2 and O_2 are gaseous and standard free energy, enthalpy and entropy changes for reaction (2.7) are:

$$\begin{aligned} \Delta G_d^\circ(\text{H}_2\text{O}) &= +237.22 \text{ kJ mol}^{-1} \Rightarrow E^\circ = \frac{\Delta G_d^\circ(\text{H}_2\text{O})}{2F} = 1.2293 \text{ V} \approx 1.23 \text{ V} \\ \Delta H_d^\circ(\text{H}_2\text{O}) &= +285.840 \text{ kJ mol}^{-1} \Rightarrow V^\circ = \frac{\Delta H_d^\circ(\text{H}_2\text{O})}{2F} = 1.4813 \text{ V} \approx 1.48 \text{ V} \\ \Delta S_d^\circ(\text{H}_2\text{O}) &= +163.15 \text{ J mol}^{-1} \text{ K}^{-1}. \end{aligned}$$

It should be noted that the electrolysis of water vapour in standard conditions (this is a fictitious state because liquid water is stable in such conditions) is less than the value for liquid water:

$$\Delta G_d^\circ(\text{H}_2\text{O}(\text{vap})) = +241.80 \text{ kJ mol}^{-1} \Rightarrow E^\circ = \frac{\Delta G_d^\circ(\text{H}_2\text{O})}{2F} \approx 1.18 \text{ V}.$$

2.1.4

pH Dependence of Water Dissociation Voltage

In acidic media, half-cell reactions are given by Equations 2.5 and 2.6. On the anodic side, using the Nernst equation, one obtains:

$$E^+ = E_{\text{H}_2\text{O}/\text{O}_2}^\circ + \frac{R_{\text{PG}} T}{nF} \text{Ln} \frac{(a_{\text{H}^+})^2 (f_{\text{O}_2}^{1/2})}{a_{\text{H}_2\text{O}}} \quad (2.12)$$

where a_{H^+} is the activity of protons in the electrolyte phase; f_{O_2} is the fugacity of oxygen in the anodic compartment and $a_{\text{H}_2\text{O}}$ is the activity of water.

A simplified but still accurate expression can be obtained using the following simplifying assumptions:

- The acidic electrolyte is sufficiently diluted to assume that the activity coefficient of protons is close to unity; therefore, their activity is equal to their molar concentration and simply related to pH.
- Pure oxygen is evolved during electrolysis (effect of saturated water vapour is neglected) and fugacity is equal to partial pressure, which is equal to 1 bar.
- Activity of water is close to unity because the electrolyte is diluted (in 1 M proton solutions, there is 98% of water molecules).

On the basis of these three assumptions, Equation 2.12 simplifies into (the reference is the normal hydrogen electrode or NHE):

$$E^+ \approx 1.23 - 0.06\text{pH} \quad (2.13)$$

On the cathodic side:

$$E^- = E_{\text{H}_2/\text{H}^+}^\circ + \frac{R_{\text{PG}} T}{nF} \ln \frac{a_{\text{H}^+}^2}{f_{\text{H}_2}} \approx -0.06\text{pH} \quad (2.14)$$

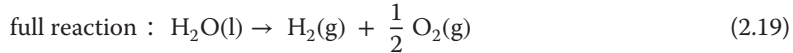
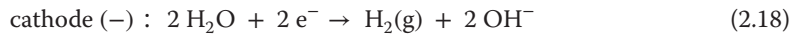
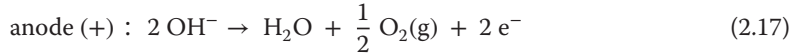
Using the same assumptions as before, at 298 K and when the pressure of hydrogen is 1 bar (ideal gas), Equation 2.14 simplifies into:

$$E^- \approx -0.06\text{pH} \quad (2.15)$$

Therefore, the cell voltage required to split water in acidic media is a constant independent of pH:

$$E_{\text{cell}} = E^+ - E^- = 1.23 \text{ V} \quad (2.16)$$

In alkaline media, the following half-cell reactions take place:



From the Nernst equation, it follows that:

$$E^+ = E_{\text{H}_2\text{O}/\text{O}_2}^\circ + \frac{R_{\text{PG}} T}{nF} \ln \frac{(a_{\text{H}_2\text{O}}) (f_{\text{O}_2}^{1/2})}{a_{\text{HO}^-}^2} \quad (2.20)$$

At 298 K, when the pressure of oxygen is 1 bar (ideal gas), Equation 2.20 simplifies into:

$$E^+ \approx 1.23 + \text{pKe} - 0.06\text{pH}$$

On the cathodic side:

$$E^- = E_{\text{H}_2\text{O}/\text{H}_2}^\circ + \frac{R_{\text{PG}} T}{nF} \ln \frac{a_{\text{H}_2\text{O}}^2}{f_{\text{H}_2} a_{\text{HO}^-}^2} \quad (2.21)$$

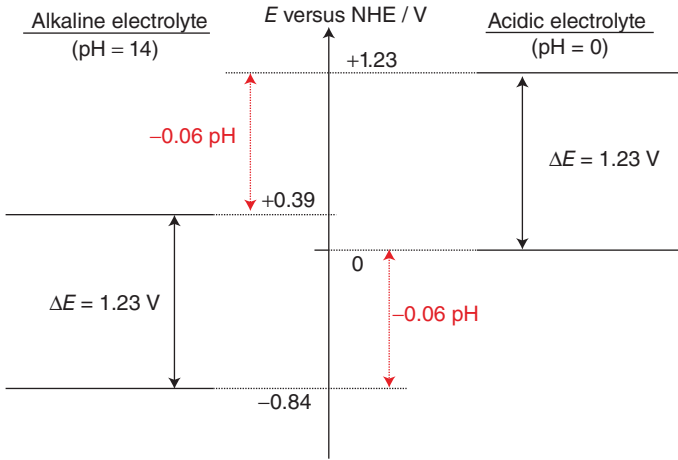


Figure 2.2 Electrode potential versus pH for the water splitting reaction.

At 298 K, when the pressure of hydrogen is 1 bar (ideal gas), Equation 2.21 simplifies into:

$$E^- \approx \text{pKe} - 0.06\text{pH} \quad (2.22)$$

Therefore, the voltage required to split water in alkaline media is:

$$E_{\text{cell}} = E^+ - E^- = 1.23 \text{ V} \quad (2.23)$$

Therefore, the free energy electrolysis voltage required to split water into hydrogen and oxygen is pH independent. The only difference between alkaline and acidic media is that the potential of each electrode is shifted along the potential axis, as a function of electrolyte pH (Figure 2.2). Consequences are mostly on electrode material stability. In acidic media, most metals are corroded and, hence, platinum group metals (PGMs) are needed. This is usually unsupported platinum or carbon-supported platinum nano-particles for the HER and iridium dioxide for the OER. In alkaline media, nickel and cobalt are passivated and oxides/hydroxides are electrochemically active.

2.1.5

Temperature Dependence of Water Dissociation Voltage

As discussed above, enthalpy, entropy and free energy changes associated with the water splitting reaction are functions of both temperature and pressure (the two main experimental parameters in water electrolysis). As a result, thermodynamic voltages (enthalpy voltage and free energy voltage) are also functions of operating temperature and pressure, as well as energy efficiencies. Accurate determination of cell efficiency requires a quantitative knowledge of temperature and pressure dependencies of thermodynamic voltages. In the following, the discussion will focus on low-temperature processes.

Table 2.1 Coefficients used in Equations 2.26 and 2.27.

Element	<i>a</i>	<i>b</i>	<i>c</i>	<i>e</i>
H ₂ (g)	26.57	3.77	1.17	—
O ₂ (g)	34.35	1.92	-18.45	4.06

Under atmospheric pressure, liquid water is electrolysed in the 0–100 °C temperature range and water vapour above 100 °C. $\Delta H(T,1)$ and $\Delta G(T,1)$ are defined as:

$$\Delta H(T, 1) = \frac{V(T, 1)}{2 F} = H_{\text{H}_2}(T, 1) + \frac{1}{2}H_{\text{O}_2}(T, 1) - H_{\text{H}_2\text{O}}(T, 1) \quad (2.24)$$

$$\Delta G(T, 1) = \frac{E(T, 1)}{2 F} = G_{\text{H}_2}(T, 1) + \frac{1}{2}G_{\text{O}_2}(T, 1) - G_{\text{H}_2\text{O}}(T, 1) \quad (2.25)$$

Enthalpy and entropy formation of H₂(g) and O₂(g) can be obtained from the following polynomial expressions (coefficients are listed in Table 2.1):

$$H_i(T, 1) - H_i^\circ = a(T - T_0) + \frac{b}{2} 10^{-3} (T^2 - T_0^2) - c 10^5 \left(\frac{1}{T} - \frac{1}{T_0} \right) - \frac{e}{2} 10^8 \left(\frac{1}{T^2} - \frac{1}{T_0^2} \right) \quad (2.26)$$

$$S_i(T, 1) - S_i^\circ = a(\ln T - \ln T_0) + b 10^{-3} (T - T_0) - \frac{c}{2} 10^5 \left(\frac{1}{T^2} - \frac{1}{T_0^2} \right) - \frac{e}{3} 10^8 \left(\frac{1}{T^3} - \frac{1}{T_0^3} \right) \quad (2.27)$$

Water enthalpy and entropy of formation are obtained from the steam tables [2]. Data are plotted in Figure 2.1. They can be used directly to calculate $E(T,1)$ and $V(T,1)$. Some empirical expressions of $V(T,P)$ and $E(T,P)$ have also been reported in the literature [3]. They apply only to the electrolysis of liquid water (for $T > 100$ °C, at a pressure sufficiently high to avoid water vapourization).

$$V(T) = 2 F \Delta H(T) = 1.485 - 1.49 \times 10^{-4} * (T - T^0) - 9.84 \times 10^{-8} * (T - T^0)^2 \quad (2.28)$$

$$E(T) = 2 F \Delta G(T) = 1.5184 - 1.5421 \times 10^{-3} * T + 9.523 \times 10^{-5} * T * \ln(T) + 9.84 \times 10^{-8} T^2 \quad (2.29)$$

$E(T)$ and $V(T)$ from Equations 2.28 and 2.29 are plotted in Figure 2.3. Trends are of course similar to those of $\Delta G(T)$ and $\Delta H(T)$. The free energy electrolysis voltage $E(T)$ decreases from 1.23 V at 25 °C down to 1.18 V at 100 °C and down to ≈ 0.9 V at 1000 °C.

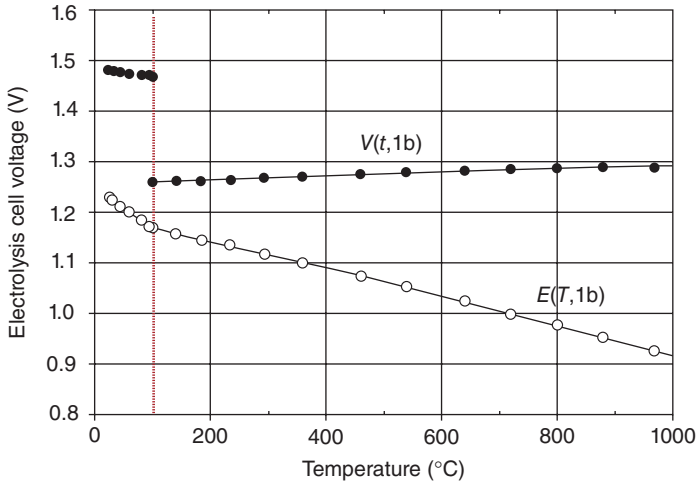


Figure 2.3 Role of operating temperature on the free energy electrolysis voltage $E(T)$ and the enthalpy electrolysis voltage $V(T)$ of water ($P = 1$ bar).

From a practical viewpoint, the maximum temperature accessible to low-temperature technology ($\approx 100\text{--}130^\circ\text{C}$) comes from material constraints and not from the vapourization of water, which can be easily managed by appropriate pressurization. In PEM technology, for instance, the maximum temperature is 90°C (as in fuel cell applications) because hydrated polymers (such as perfluorosulphonic Nafion[®] [4]) lose all mechanical stability above 100°C . Even if the domain of operating temperature can be extended up to $+150^\circ\text{C}$ using more stable materials (e.g. with short side chains materials originally developed at Dow Chemicals or PBI-based materials), high operating temperatures always negatively impact the stability and durability of membrane-electrode assemblies (MEAs) and catalytic layers.

2.1.6

Pressure Dependence of Water Dissociation Voltage

Hydrogen storage for either mobile or stationary applications is a critical issue. Among different processes, the storage of compressed hydrogen is probably the simplest and most straightforward one. Pressurized vessels that can sustain pressures as high as 700 bars are already available for application in the automotive industry. To fill such tanks with hydrogen of electrolytic grade, there are two options. The first one is to perform water electrolysis at atmospheric pressure and then to compress gaseous hydrogen up to the desired value using an external compressor. The second one is to develop pressurized water electrolyzers that can directly deliver pressurized hydrogen at the value of interest (direct electrochemical compression). Different parameters (capex, opex, efficiency) need to be considered to identify the best option. To compare the two processes

more accurately, it is necessary to evaluate the role of operating pressure on the thermodynamics and the kinetics of the water splitting reaction (taking into account the energy required for the injection of liquid water at atmospheric pressure into the pressurized electrolyser). Usually, the best solution is a hybrid one: pressurized electrolysers deliver compressed hydrogen at medium pressure value (15–50 bars) and then the target pressure is reached by mechanical compression. This is because compression energy requirements are more significant at low pressure than at elevated pressure. Although pressurized alkaline water electrolysis is commonly used in the industry (with operating pressure in the 1–50 bar range), the discussion provided in the following is mainly based on PEM water electrolysis for which prototypes operating at very high pressure (several hundred bars) have already been developed and successfully tested.

2.1.6.1 General Pressure Dependence

From basic thermodynamic considerations, the pressure dependence of the free energy electrolysis voltage E is:

$$\left(\frac{\partial E}{\partial P}\right)_T = \frac{1}{nF} \left(\frac{\partial \Delta G}{\partial P}\right)_T = \frac{\Delta \bar{V}}{nF} \quad (2.30)$$

where $\Delta \bar{V}$ is the change of molar volume associated with the compression. Considering the fact the effect of pressure on the volume of condensed phases is small, $\Delta \bar{V}$ can be written by considering only gaseous species. At low pressures, the law of ideal gases prevails (for higher pressure, more accurate state equations are required) and:

$$\Delta \bar{V} = \sum_i v_i \frac{R_{PG} T}{p_i} \quad (2.31)$$

where p_i is the partial pressure of species i and v_i is the stoichiometric factor. Therefore:

$$\left(\frac{\partial E}{\partial P}\right)_T = \sum_i v_i \frac{R_{PG} T}{nF p_i} \equiv \sum_i \left(\frac{\partial E}{\partial p_i}\right)_T \quad (2.32)$$

Integration of Equation 2.32 gives:

$$E = E^\circ + \sum_i v_i \left(\frac{R_{PG} T}{nF}\right) \text{Ln} \left(\frac{p_i}{p^\circ}\right) \quad (2.33)$$

Application of Equation 2.33 to water electrolysis yields:

$$E = E^\circ + \frac{R_{PG} T}{2F} \text{Ln} \left(\frac{p_{H_2}}{p^0} \cdot \sqrt{\frac{p_{O_2}}{p^\circ}}\right) \quad (2.34)$$

Let P be the pressure of operation (PEM cells can be operated under a difference of pressure but this case is not considered here). In the case of water electrolysis (almost) pure hydrogen and oxygen are evolved in each compartment. Main impurities are water (saturation at the temperature T of operation), traces of oxygen in hydrogen and of hydrogen in oxygen due to cross-permeation effects and traces

of KOH in the alkaline process. Neglecting the effect of these impurities, then $p_{\text{O}_2} = P$ at the anode and $p_{\text{H}_2} = P$ at the cathode, and the following relationship is obtained:

$$E = E^\circ + \frac{3R_{\text{PG}}}{4F} T \ln(P) \quad (2.35)$$

When the electrolysis pressure changes from P_1 to P_2 , then the cell voltage changes by ΔE :

$$\Delta E = \frac{3}{4F} R_{\text{PG}} T \ln\left(\frac{P_2}{P_1}\right) \quad (2.36)$$

In Equation 2.36, setting the reference pressure P_1 at 1 bar, one obtains:

$$E(T, P) = E(T, 1) + \frac{3}{4} \frac{R_{\text{PG}}}{F} T \ln(P) \quad (2.37)$$

The free energy voltages (E) calculated from Equation 2.37 for different operating pressures at 298 and 373 K are plotted in Figure 2.4. More accurate calculations can be made using more elaborated state equations, in particular at pressures above 10 bars, when significant differences appear with the law of ideal gas [5]. Figure 2.4 shows that the additional energy cost due to electrochemical compression (approximately 120 mV at 298 K from 1 to 60 bars) remains significantly less than charge transfer overvoltages which appear during operation at high current density (especially the anodic overvoltage of approximately 400–800 mV at 1 A cm⁻²). This is why electrochemical compression is attracting interest, although the impact on capex can be quite significant.

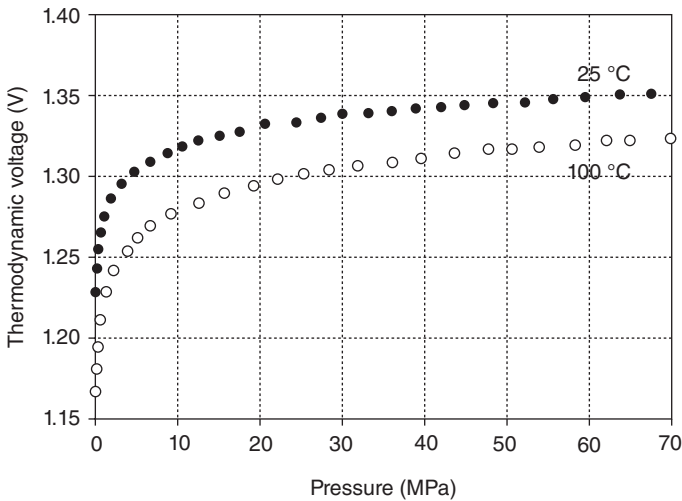


Figure 2.4 Plot of the free energy voltage of water electrolysis as a function of pressure for three different operating temperatures. Data based on the assumption of ideal gases.

2.1.6.2 Detailed Pressure Dependence

Equation 2.37 provides a simple and good approximation for $E(T,P)$ for low pressures (<10 bars). More accurate calculations are required using more elaborated state equations for operating pressure above 10–15 bars. Such expressions can be obtained from the values of $V(298,1)$ and $E(298,1)$ as follows.

$$\Delta H(T,P) = H_{\text{H}_2}(T,P) + \frac{1}{2}H_{\text{O}_2}(T,P) - H_{\text{H}_2\text{O}}(T,P) \quad (2.38)$$

$$\Delta S(T,P) = S_{\text{H}_2}(T,P) + \frac{1}{2}S_{\text{O}_2}(T,P) - S_{\text{H}_2\text{O}}(T,P) \quad (2.39)$$

$$\Delta G(T,P) = \Delta H(T,P) - T.\Delta S(T,P) = G_{\text{H}_2}(T,P) + \frac{1}{2}G_{\text{O}_2}(T,P) - G_{\text{H}_2\text{O}}(T,P) \quad (2.40)$$

$H_i(T,P)$, $S_i(T,P)$ and $G_i(T,P)$ values are obtained in two steps, first by calculating the effect of temperature at constant pressure of 1 bar, then by calculating the pressure effect at target temperature:

$$H_i(T,P) = [H_i(T,P) - H_i(T,1)] - [H_i(T,1) - H_i(298,1)] \quad (2.41)$$

$$S_i(T,P) = [S_i(T,P) - S_i(T,1)] - [S_i(T,1) - S_i(298,1)] \quad (2.42)$$

$$G_i(T,P) = [G_i(T,P) - G_i(T,1)] - [G_i(T,1) - G_i(298,1)] \quad (2.43)$$

Enthalpy and entropy of $\text{H}_2(\text{g})$ and $\text{O}_2(\text{g})$ formation under 1 bar pressure are obtained from Equations 2.26 and 2.27. Enthalpy and entropy of $\text{H}_2\text{O}(\text{l})$ formation under 1 bar pressure are obtained from the steam tables [2]. The role of operating pressure is taken into account as follows. Usually, the classical virial expansion (introduced in 1901 by H. Kamerlingh Onnes as a generalization of the ideal gas law) is used to express the pressure of a many-particle system at equilibrium as a power series in the density. Virial coefficients B_i appear as coefficients in the virial expansion of the pressure, thus providing systematic corrections to the ideal gas law. They are characteristic of the interaction potential between the particles and in general depend on the temperature. The second virial coefficient depends only on the pair interaction between the particles, the third depends on two- and non-additive three-body interactions and so on. The pressure change of ΔH and ΔG is given by the following state equations:

$$H(T,P) - H(T,1) = \left(B - T \frac{\partial B}{\partial T} \right) P + \frac{C - B^2 - 0.5 T \left[\frac{\partial C}{\partial T} - 2 B \frac{\partial B}{\partial T} \right]}{R_{\text{PG}} T} P^2 \quad (2.44)$$

$$G(T,P) - G(T,1) = R_{\text{PG}} T \ln P + B P + \frac{C - B^2}{2 R_{\text{PG}} T} P^2 \quad (2.45)$$

The virial constant B and C can be approximated as function of temperature:

$$B = b_1 + \frac{b_2}{T} \quad (\text{cm}^3 \text{ mol}^{-1}) \quad (2.46)$$

Table 2.2 Coefficients used in Equations 2.46–2.49.

Compound	b_1	b_2	c_1	c_2
H ₂ (g)	20.5	-1857	-351	12760
O ₂ (g)	42.6	-17400	-2604	61457

$$C = c_1 + \frac{c_2}{T^{\frac{1}{2}}} \quad (\text{cm}^6 \text{ mol}^{-2}) \quad (2.47)$$

$$\frac{dB}{dT} = -\frac{b_2}{T^2} \quad (\text{cm}^3 \text{ mol}^{-1} \text{ K}^{-1}) \quad (2.48)$$

$$\frac{dC}{dT} = -\frac{c_2}{T^{\frac{3}{2}}} \quad (\text{cm}^6 \text{ mol}^{-2} \text{ K}^{-2}) \quad (2.49)$$

H₂(g) and O₂(g) coefficients of virial constant for pressures up to 1000 atm are shown in Table 2.2:

Enthalpy and entropy changes of H₂O(l) with pressure are obtained from the steam tables. $E(T,P)$ and $V(T,P)$ obtained from the above set of equations are plotted on Figures 2.5 and 2.6 at different operating temperatures [5].

A comparison of Figures 2.4 and 2.5 shows that the ideal gas assumption is useful to approximate the effect of pressure on the free energy voltage but not sufficient for accurate determination. Although the effect of pressure on the free energy voltage E is significant (+200 mV at 25 °C when the pressure is raised from 1 to

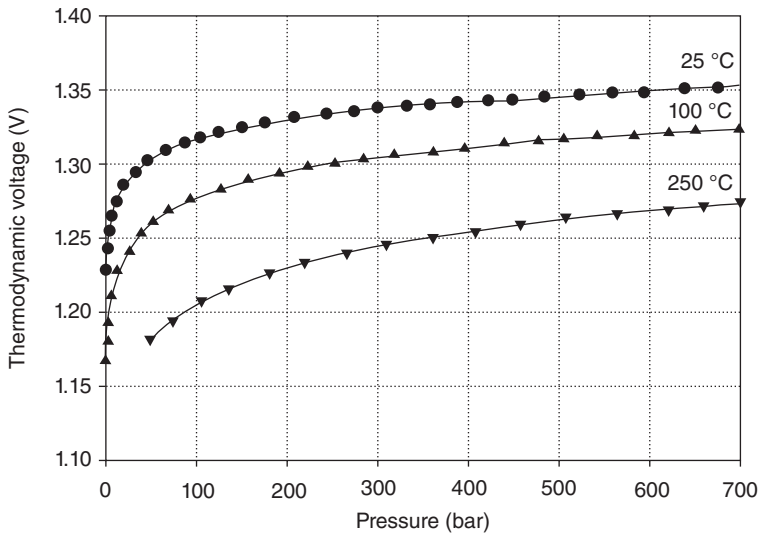


Figure 2.5 Plot of the free energy voltage $E(P)$ of water electrolysis as a function of pressure for three different operating temperatures.

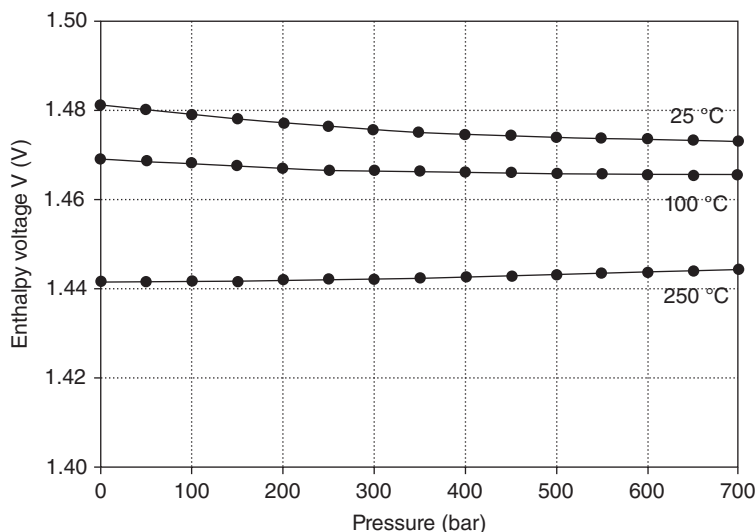


Figure 2.6 Plot of the enthalpy voltage $V(P)$ of water electrolysis as a function of pressure for three different operating temperatures.

700 bar), its effect on the enthalpy voltage V remains limited. The main conclusion from these more accurate data is the confirmation that the energy cost of electrochemical compression is very limited and remains significantly less than charge transfer overvoltages which appear during operation at high current density.

2.2

Efficiency of Electrochemical Water Splitting

2.2.1

Water Splitting Cells: General Characteristics

Electrolysers are devices used to perform endergonic transformations (non-spontaneous chemical reactions that absorb energy in the form of electrical work). Electrolysers contain several (up to hundreds) series-connected elementary electrolysis cells (usually filter-press configuration is preferred to increase compactness and reduce parasite ohmic losses). An electrolysis cell is basically a galvanic chain of planar geometry containing two metallic electrodes placed face to face and clamping a thin electrolytic layer (ions dissolved in liquid polar solvents or ion-conducting polymers or oxygen ion-conducting ceramic). In such electrochemical chains, there are two metal/electrolyte interfaces placed in series. During operation, a continuous current flows across the cell. In the external circuit up to the electrodes, the charge carriers are the electrons, and in the electrolyte, the charge carriers are mobile ions. Electrons can cross interfaces and induce redox transformations of interest (oxygen and hydrogen evolution

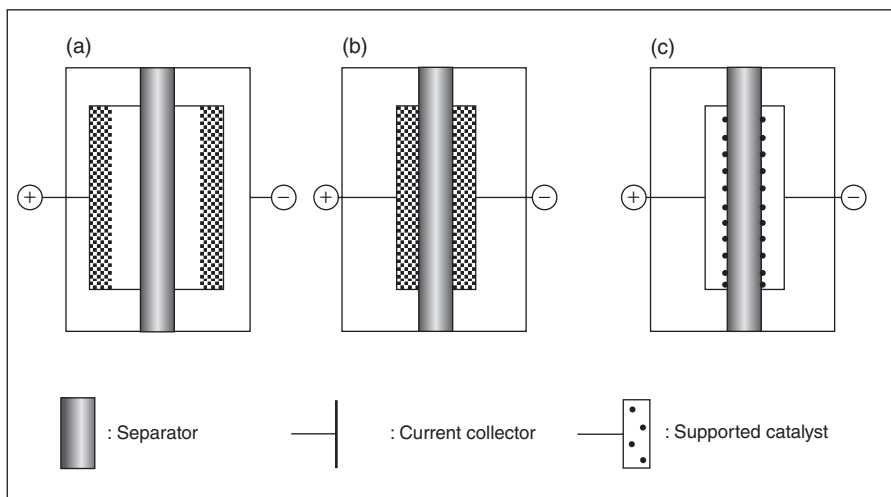


Figure 2.7 Two-dimensional schematic diagrams of (a) a gap cell; (b) a zero-gap cell and (c) a SPE (solid polymer electrolyte) cell.

in the case of water electrolysis). Basically, three different cell concepts are used in industrial devices (Figure 2.7). The first concept (Figure 2.7a) is called a ‘*gap cell*’. This is the most conventional and simple configuration in which two planar electrodes (usually a cheap electron-conducting substrate surface-covered by a thin layer of a more expensive electrocatalyst) are placed face to face in a liquid electrolyte. A separator (usually a porous diaphragm impregnated with the electrolyte) is introduced in the interpolar gap to prevent the spontaneous recombination of reaction products. In the case of water electrolysis, bubbles of gaseous species form at each interface. The distance between electrodes and diaphragm must be sufficiently large to let gases evolve freely but not too large to reduce ohmic losses. When bubble concentration increases, there is a tendency to form continuous and highly resistive gaseous films over electrode surfaces and therefore the maximum operating current density is usually limited (several hundred mA cm^{-2}) in this kind of cell. The situation can be somewhat improved using the second concept of cell (so-called ‘*zero-gap cell*’ shown in Figure 2.7b), which is more appropriate for gas-evolving electrodes. In such cells, porous electrodes are pressed directly onto the separator, to reduce as much as possible the distance between the anode and the cathode (and corresponding ohmic losses). Gaseous products are released through the pores at the backside. Significantly larger current densities can be reached without significant extra voltage losses. The concept is used in advanced and modern alkaline water electrolyzers. However, a liquid electrolyte is still needed and this cell design is not appropriate for operation in acidic media. The third concept is called a ‘*PEM cell*’ (Figure 2.7c). PEM stands for proton exchange membrane or polymer electrolyte membrane. The cell separator is a thin ion-conducting polymeric film that is used for the double purpose of conveying electric charges (protons in the case of PEM water electrolysis) from the

anode to the cathode and separating gas products. There is no liquid electrolyte in circulation in this kind of cell. This concept was first proposed for H_2/O_2 fuel cells in the 1950s, at the dawn of the US space programme, to solve the problems associated with the operation of electrochemical cells in a low-gravity environment and those due to the corrosion of metals in acidic media. The idea was used latter for the development of water electrolyzers. In a PEM water electrolysis cell, porous catalytic layers are coated on each side of the membrane surface. Electric contacts are obtained by pressing porous current collectors on each side. There is no liquid electrolyte. Only de-ionized water is circulated in the anodic chamber to feed the electrochemical reaction. The same concept of cell is used at high temperature, the separator and electrolyte being a thin oxide-ion-conducting ceramic membrane.

It should be noted that, although more efficient than a liquid electrolyte cell, the PEM cell concept adds more geometrical constraints. In a zero-gap cell using a liquid electrolyte (water electrolysis alkaline technology), there is no need to accurately adjust the distance between cell components: the liquid electrolyte fills the entire interpolar region and ensures a homogeneous distribution of current lines. In a PEM cell, the situation is different. The electrolyte is confined inside the membrane. There is a need to adjust the thickness, surface state, dimension and position of all cell components very accurately. There is also a need to pay significant attention to the mechanics of the stack in order to ensure homogenous distributions of compression forces that are critically required for homogeneous distribution of current lines. This difference also contributes to make polymer electrolyte technology more expensive.

2.2.2

Main Sources of Energy Dissipation in Electrochemical Cells

The most significant part (>60%) of electricity supplied to an electrolysis cell is used for the Gibbs free energy change of the endergonic transformation of interest. However, there are several sources of energy degradation (electricity into heat) in a water electrolysis cell. Their magnitude and localization depend on the cell design. Figure 2.8 shows the cross section of a gap cell with liquid electrolyte and the associated distribution of electric potential during operation. Potential drops are located inside bulk electrodes due to internal resistance (1, 1'), across electroactive layers which are not always good electronic conductors (2, 2'), at interfaces where charge transfer processes take place (3, 3'), in solution, across the diffusion layers close to the electrode surface when mass transport phenomena are involved or gaseous species are formed (4, 4'), by transport of ions in the bulk electrolyte (5, 5') and across the cell separator (6). A similar situation is found in zero-gap and in PEM cells.

Figure 2.9 shows the general shape of the polarization curve measured during water electrolysis at 25 °C, under 1 bar pressure. The free energy electrolysis voltage is 1.23 V. This is usually the most significant voltage contribution. Above this voltage value, current starts to flow across the cell. Additional electric power is

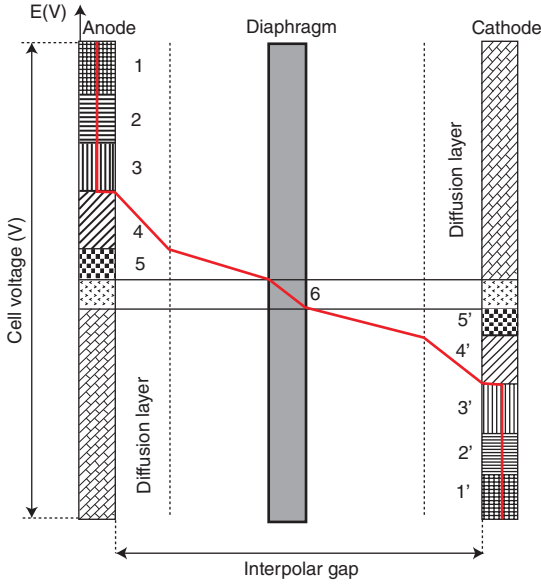


Figure 2.8 Schematic diagram of potential distribution in a gap cell water electrolysis cell.

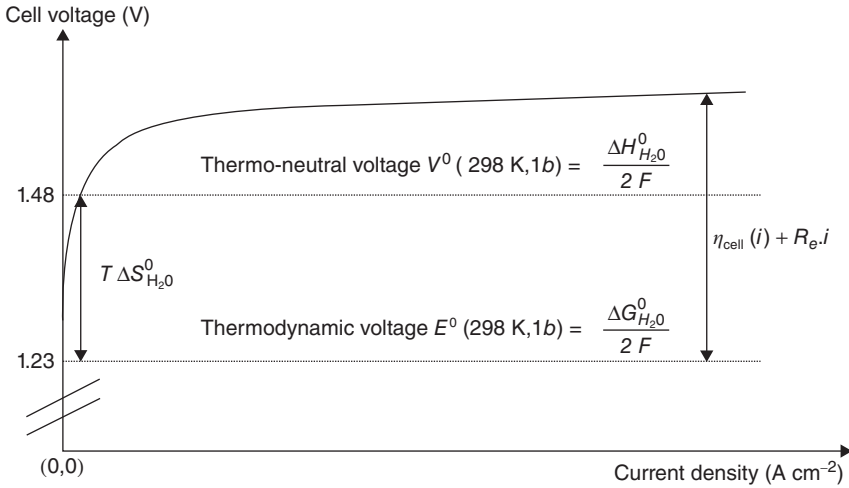


Figure 2.9 Schematic diagram of a water electrolysis polarization curve.

used to overcome some internal resistances and electricity is dissipated as heat to the surroundings. At low current densities, ohmic voltage drops are small whereas charge transfer overvoltages are maximum. The logarithmic shape of the polarization curve is due to these charge transfer phenomena at the anode and the cathode. In the case of water electrolysis, the anodic overvoltage is significantly larger than the cathodic one because the kinetics of the OER is much lower than that of the

HER. Then, as the current density increases, charge transfer resistances decrease and the shape of the polarization curve becomes linear. The shape is dictated by the ohmic resistance of the cell (sum of electronic and ionic resistances) which is therefore a key kinetic parameter. This is especially true in industrial systems of large surface areas where parasite ohmic losses can have a very negative impact on the energy consumption of the cell, especially in PEM cells where there is no liquid electrolyte. Additional parasitic ohmic losses can appear due to inadequate electric contacts between cell components (bipolar plates, current collectors, etc.). This can ultimately lead to unacceptable cell voltages. The quality of an electrolyser must be appreciated by its energy efficiency and its ability to maintain good electrochemical performances on the long term (in the upper range of the $10^4 - 10^5$ h time interval).

It should be noted that when the operating current density is such that Equation 2.50 is satisfied:

$$2F (\eta_{\text{cell}} + R_e \cdot i) = T \Delta S_d \quad (2.50)$$

then there is no need to transfer heat from the surroundings to the electrolysis cell. This is the reason why the operating point $V_d(T, P) = \Delta G_d/2F + T \Delta S_d/2F = \Delta H_d/2F$ is called the ‘thermo-neutral electrolysis voltage’ of the cell.

2.2.3

Energy Efficiency of Water Electrolysis Cells

In water electrolysis cells, the theoretical amount of energy W_t required to split 1 mole of water at (T, P) is given from thermodynamic calculations. However, thermodynamics pertains to equilibrium conditions. To reduce capex, there is a need to operate the cells at high current densities. As the current density increases, an increasing share of the electrical work provided to the cell is degraded into heat. This is a source of inefficiency and increasing opex. From a practical viewpoint, capex and opex must be balanced and a current density of 1 A cm^{-2} is a good reference value. Electronic conductivity, charge transfer processes at interfaces and ionic transport in the electrolyte are the three main sources of energy degradation.

The efficiency of a water electrolysis cell measures the ratio of the theoretical amount of energy W_t to the real amount of energy W_r required to split 1 mole of water. Because of heat degradation, $W_r > W_t$. The cell efficiency is defined as:

$$\varepsilon = \frac{W_t}{W_r} \quad (2.51)$$

where $W_r = (U_{\text{cell}} \cdot I \cdot t)$, U_{cell} is the actual cell voltage in volts, I is the current in amperes and t is the duration in seconds. W_t can be defined from the free energy voltage E : $W_{t,\Delta G} = (E \cdot I \cdot t)$. W_t can also be defined from the thermo-neutral voltage V : $W_{t,\Delta H} = (V \cdot I \cdot t)$.

Therefore, two different definitions can be used to calculate the efficiency of a water electrolysis cell. Because E and V are both functions of operating temperature T and operating pressure P and because U_{cell} is also a function of the

operating current density j , the two different cell efficiencies can also be expressed as a function of T , P and j :

$$\varepsilon_{\Delta G}(T, P, j) = \frac{E(T, P)}{U_{\text{cell}}(T, P, j)} \quad \varepsilon_{\Delta H}(T, P, j) = \frac{V(T, P)}{U_{\text{cell}}(T, P, j)} \quad (2.52)$$

At low current densities, cell efficiencies close to 100% are obtained. Efficiency tends to decrease when current density increases. For example, in conventional PEM water electrolyzers, $\varepsilon_{\Delta H} \approx 70\%$ at 1 A cm^{-2} , $T = 90^\circ\text{C}$ and $P = 1 \text{ bar}$.

Finally, it should be noted that in low-temperature water electrolysis technology, liquid water is electrolysed and the electrical efficiency should be calculated using the high heating value of the reaction. In high-temperature technology, water vapour is electrolysed and the electrical efficiency should be calculated using the low heating value of the reaction. One interested of high temperature water electrolysis is that waste heat sources can be used for the vapourization of water.

2.2.4

Faradaic Efficiency of Water Electrolysis Cells

The faradaic efficiency ε_F is used to measure the efficiency of current flowing across the cell. The faradaic efficiency of each interface can be measured separately. In water electrolysis cells, the relationship between the current and the chemical gas production at each electrode is defined as:

$$(\varepsilon_F)^{\text{anodic}} = F \frac{(dn_{\text{O}_2}/dt)}{i} \times 100 \quad (2.53a)$$

$$(\varepsilon_F)^{\text{cathodic}} = F \frac{(dn_{\text{H}_2}/dt)}{i} \times 100 \quad (2.53b)$$

Ideally, ε_F should be as close as possible to unity. In water electrolysis cells, gaseous species are formed at both anodic (oxygen) and cathodic (hydrogen) interfaces. It is necessary to collect them separately and to avoid their spontaneous recombination by interdiffusion in the inter-polar area. Spontaneous chemical recombination would release the Gibbs free energy change as heat which is a source of inefficiency for the electrical work transferred to the cell. Separators are used to prevent hydrogen/oxygen recombination. In alkaline water electrolysis cell, the separator is an electrolyte-impregnated diaphragm (asbestos was used until it was banned for safety reasons and replaced by various polymeric materials [6, 7]). In PEM water electrolysis cell, the separator is the polymer membrane (a biphasic organic/water material made of water-impregnated perfluorinated perfluorosulphonic polymer). In high-temperature water electrolysis, the separator is an oxide-ion-conducting ceramic.

Ideally, cell separators should be totally gas-proof. In real situations, the solubility of gases (hydrogen and oxygen) in the electrolyte is usually limited but not zero. Mass transport occurs across the separator, especially at high current density and/or high operating pressure. For example, both gases are soluble in aqueous KOH solution and the porous diaphragm is somewhat permeable. The same is true

of the polymer electrolyte in PEM cells whereas pinhole-free ceramics are less prone to interdiffusion of gases. As a consequence, hydrogen can diffuse across the separator from the cathode to the anode and oxygen from the anode to the cathode, the flow being proportional to their respective diffusion coefficients in the media. Hydrogen reaching the anodic compartment can either react chemically with oxygen or be e-oxidized at the anode. Symmetrically, the oxygen reaching the cathodic compartment can react with gaseous or dissolved hydrogen or can be electrochemically reduced at the cathode. From a global viewpoint, this is as if a parasitic current was decreasing the chemical or faradaic efficiency of the cell. Faradaic efficiencies must be measured to optimize cell design and improve cell efficiency.

2.3

Kinetics of the Water Splitting Reaction

In the absence of mass transport limitations, the kinetics of charge transfer processes at any metal/electrolyte interface follows the so-called Butler–Volmer relationship [8]:

$$i = \vec{i} + \overleftarrow{i} = i_0 \left\{ \exp \left[\frac{\beta n F}{R T} \eta \right] - \exp \left[-\frac{(1 - \beta) n F}{R T} \eta \right] \right\} \quad (2.54)$$

where i_0 is the exchange current density (in A cm^{-2}) of the half-cell process considered; β is the symmetry factor [9]; $n = 2$ is the number of electrons exchanged during the electrochemical splitting of one water molecule; $F \approx 96\,485 \text{ C mol}^{-1}$ is the Faraday constant, that is, the electric charge of 1 mole of electrons; $R = 8.314 \text{ J mol}^{-1} \text{ K}^{-1}$ is the constant of perfect gas, η is the charge transfer overvoltage (in V) and T is the absolute temperature in Kelvin.

According to Equation 2.54, the main kinetic parameter which determines the efficiency of charge transfer processes is the exchange current density i_0 , which is an intensive physical property. The higher the current density, the more reversible is the reaction and the more efficient the charge transfer process. The best electrocatalysts are those having the higher exchange current density for the half-cell reaction of interest. Exchange current densities are expressed per unit surface of geometrical electrode/electrolyte interface. It should be noted that apparent exchange current densities can be increased by developing rough (three dimensions) interfaces.

2.3.1

Half-Cell Reaction Mechanism in Acidic Media

2.3.1.1 HER

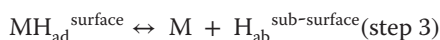
The mechanism of HER in acidic media has been extensively studied in the early days of both experimental and theoretical electrochemistry because this is a highly reversible reaction that can be used to set in a very reproducible way the electrode potential. On the basis of the extended work of pioneering electrochemists such

Table 2.3 Two main HER mechanisms on Pt in acidic media.

Mechanism 1	Mechanism 2
$H^+ + 1 e^- + M \leftrightarrow MH_{ad}^{surface}(\text{step 1})$	$H^+ + 1 e^- + M \leftrightarrow MH_{ad}^{surface}(\text{step 1})$
$2 MH_{ad}^{surface} \leftrightarrow H_2(g) + 2 M(\text{step 2})$	$H^+ + 1 e^- + MH_{ad}^{surface} \leftrightarrow H_2(g) + M(\text{step 2}')$

as Frumkin, Conway and Parsons, only two reactions paths involving two steps each are now regarded as likely to occur in acidic media, as described in Table 2.3 where H_{ad} denotes a surface-adsorbed hydrogen ad-atom:

H_{ad} species are formed by proton electronation (Volmer step 1). Molecular hydrogen (gaseous) evolves either by direct chemical recombination of surface hydrogen ad-atoms (Tafel step 2) or by electrochemical recombination (Heyrovsky step 2'). When Pd or Pd-based materials are used as electrocatalysts [10], the HER is in competition with the hydrogen insertion reaction (HIR) that brings two additional reaction steps:



where H_{ab} denotes absorbed hydrogen atoms in subsurface regions. Fully hydrided Pd particles are also good HER catalysts. According to Frumkin [11], steps (1) and (3) form one single step whereas according to Bockris *et al.* [12], they are separate steps. On platinum, in acidic media, there is a general agreement that the HER mechanism is that of fast proton discharge followed by rate-determining chemical desorption (mechanism 1). The exchange current density of the HER on Pt in acidic media is $10^{-3} \text{ A cm}^{-2}$. The situation is similar at the cathode of PEM cells [13, 14], even when carbon-supported Pt nano-particles are used in place of bulk Pt particles: the mean diffusion path of surface H adatoms is limited to the nanometre scale due to the geometry of the catalytic powder, and carbon superficial diffusion is unlikely to happen due to strong carbon–hydrogen interactions and low H diffusivity.

2.3.1.2 OER

Many different mechanisms have been reported in the literature to account for the kinetics of the OER in acidic media on metallic oxides [15]. The most often quoted are (Table 2.4):

On Pt electrodes, mechanism 1 usually prevails. Experimental transfer coefficients for the OER and the oxygen reduction reaction (ORR) at high current density are both close to 0.5 (corresponding to a Tafel slope of $118 \text{ mV} \cdot \text{decade}^{-1}$ at 25°C and $130 \text{ mV} \cdot \text{decade}^{-1}$ at 80°C) [16]. With four electrons exchanged in the overall reaction, this corresponds to a stoichiometric number $\nu = 4$, a value consistent with mechanism 1, the first step being rds. However, Pt is not a good catalyst for the OER (and is thus never used for application in PEM

Table 2.4 Two main OER mechanisms on Pt and IrO₂ (S = reacting site).

Mechanism 1: oxide path (Pt)	Mechanism 2: Krasil'shchikov path (IrO ₂)
4 Pt + 4 H ₂ O → 4 PtOH + 4 H ⁺ + 4e ⁻ (step 1)	S + H ₂ O → S - OH + H ⁺ + 1 e ⁻ (step 1)
4 PtOH → 2 PtO + 2 PtH ₂ O (step 2)	S - OH → S - O ⁻ + H ⁺ (step 2)
2 PtO → O ₂ + 2 Pt (step 3)	S - O ⁻ → S - O + e ⁻ (step 3)
	S - O → S + $\frac{1}{2}$ O ₂ (step 4)

water electrolysis cells), the exchange current density (approximately 10⁻⁹ A cm⁻² per cm² of real interface area) being far too small. Iridium metal or iridium oxides are known as the best OER promoters in acidic media. The exchange current density measured on smooth iridium electrodes is approximately 1000 times higher ($\approx 10^{-6}$ A cm⁻² per cm² of real interface area) [17] than on Pt. According to the literature, this is the Krasil'shchikov path of Table 2.4 [18] which is most frequently found to occur on iridium oxide electrodes [19, 20].

2.3.1.3 Kinetics

Tafel parameters for low-temperature (up to 80 °C) HER and OER in acidic media using PGM catalysts are compiled in Tables 2.5 and 2.6. When current densities are corrected for the roughness of the electrodes, their values are similar to those measured on smooth electrodes.

On the basis of the data of Tables 2.5 and 2.6, the overvoltage–current density relationships for the HER and the OER on smooth PGM surfaces calculated from Equation 2.57 are plotted in Figure 2.10. Curves for the hydrogen oxidation reaction (HOR) and the ORR corresponding to the fuel cell mode are also plotted for comparison. While the shapes of the curves along the potential axis are dictated by the exponential terms of Equation 2.57, the magnitude of the overvoltage is only due to the value of the exchange current density for each reaction.

Table 2.5 Tafel parameters for hydrogen evolution reaction [12, 21, 22].

Electrode (°C)	$d\eta^{\text{cathodic}}/d(\log i)$ (mV)	α	Measured i_0 (A cm ⁻²) (geometrical area)	Measured i_0 (A cm ⁻²) (real area)	Roughness factor
Pt					
25	125	0.54	0.17	8×10^{-4}	213
80	105	0.45	0.14	8×10^{-4}	175
Pd					
25	—	0.54	—	1×10^{-3}	—
80		0.45		1×10^{-3}	

Table 2.6 Tafel parameters for oxygen evolution reaction.

Electrode (°C)	$d\eta^{\text{anodic}}/d(\log i)$ (mV)	α	Measured i_0 (A cm ⁻²) (geometrical area)	Measured i_0 (A cm ⁻²) (real area)	i_0 (A cm ⁻²) [17]
Pt					
25	110	0.54	1×10^{-7}	6×10^{-10}	1×10^{-9}
80	130	0.45	2×10^{-5}	1×10^{-7}	—
Ir					
25	110	0.54	2×10^{-4}	1×10^{-6}	1×10^{-6}
80	130	0.45	6×10^{-3}	4×10^{-5}	—

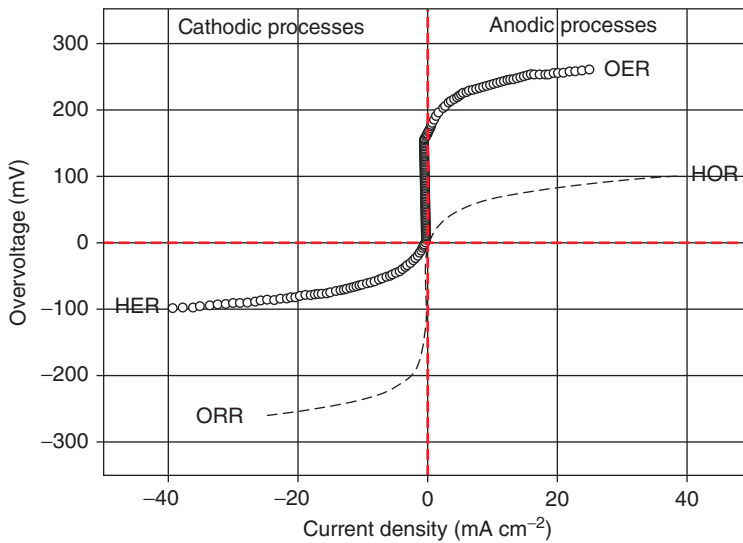


Figure 2.10 Overvoltage–current density relationships on smooth surfaces for: OER = oxygen evolution reaction on Ir^o; HER = hydrogen evolution reaction on Pt^o; ORR = oxygen reduction reaction on Pt^o and HOR = hydrogen oxidation reaction on Pt^o.

During water electrolysis, the HER overvoltage remains low whereas the OER overvoltage is larger (Figure 2.11). The relationship between η^+ (the anodic overvoltage) and η^- (the cathodic overvoltage) at any given current density i^* sufficiently large to neglect the reverse term is obtained from Equation 2.54:

$$\frac{\eta^+}{\eta^-} = \frac{\text{Ln}(i^*/i_0^+)}{\text{Ln}(i^*/i_0^-)} \quad (2.55)$$

whereas $i_0(\text{HER})/i_0(\text{OER}) \approx 1000$, $\eta^+/\eta^- \approx 2.0$ at 1 A cm^{-2} using smooth interfaces.

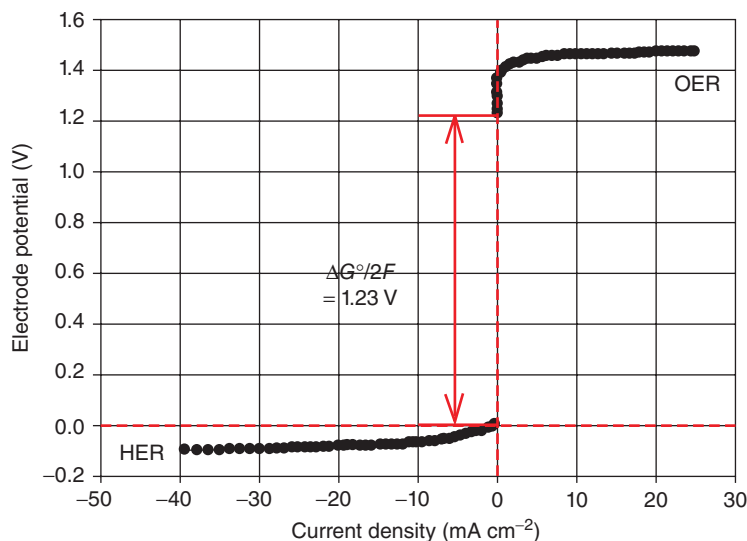
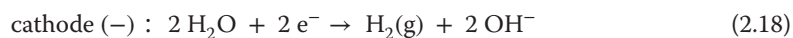
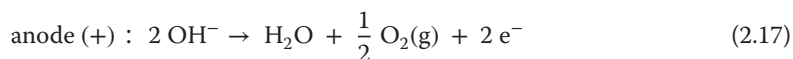


Figure 2.11 Overvoltage–current density relationship calculated at 25 °C from Equation 2.54 for the water splitting reaction in acidic media on smooth Pt and Ir surfaces.

2.3.2

Half-Cell Reaction Mechanism in Alkaline Media

In alkaline water electrolyzers, nickel is commonly used as the electrode material. Half-cell reactions are:



The exchange current density of the HER on smooth Ni foils in alkaline media at 25 °C is $i_0 \approx 7.4 \times 10^{-6} \text{ A cm}^{-2}$ [23]. Using 3D electrodes (e.g. fresh Ni-coated carbon fibres in 30 wt% KOH at 60 °C [24]), values in the $40\text{--}50 \times 10^{-6} \text{ A cm}^{-2}$ range have been obtained, corresponding to a roughness factor of approximately 7.

Some reference data for an alkaline water electrolyser are provided in Figure 2.12. The performance of some commercial alkaline water electrolyzers are compiled in Table 2.7.

2.3.3

Role of Operating Temperature on the Kinetics

As discussed above, the HER is a fast process but the OER is more sluggish at low temperature. The H^+/H_2 redox system is fully reversible but the $\text{H}_2\text{O}/\text{O}_2$ redox system is not. The situation appears more clearly by plotting on the same graph the polarization curves of a water electrolyser and a fuel cell at two different temperatures (Figure 2.13). At 90 °C, the kinetic features of the

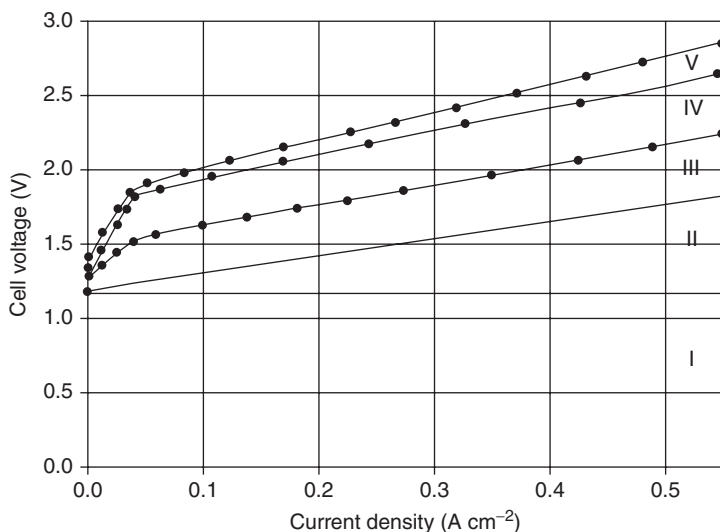


Figure 2.12 Electrochemical performances of a conventional alkaline 'membrane cell' water electrolyser at 90 °C. (I) Thermodynamic voltage (1.18 V); (II) ionic ohmic drop across electrolyte; (III) anodic (O₂) overvoltage; (IV) cathodic (H₂) overvoltage and (V) electronic ohmic drop of electrodes.

Table 2.7 Main characteristics of some commercial alkaline water electrolysers.

Manufacturer (model)	H ₂ production (Nm ³ h ⁻¹)	Production pressure (bar)	Total power (kW)	Energy system (kWh Nm ⁻³)	Energy electrolyser (kWh Nm ⁻³)	Efficiency (%)
Stuart (IMET 1000)	60	25	290	4.8	4.2	73
Teledyne (EC 750)	42	4-8	235	5.6	—	63
Proton (Hogen 380)	10	14	63	6.3	—	56
Norsk Hydro (5040)	485	30	2330	4.8	4.3	73
Avalence (Hydrofiller 175)	4.6	Up to 700	25	5.4	—	64

water/hydrogen/oxygen system are those of a poorly reversible system. The current requires a significant voltage change (≈ 500 mV) to see its sign changing and to shift from water electrolysis to fuel cell operation. Despite the fact that the equilibrium voltage is decreasing with temperature (from about 1.23 V at 90 °C corresponding to $\Delta G = 238$ kJ mol⁻¹ down to about 0.9 V at 1000 °C corresponding to $\Delta G = 177$ kJ mol⁻¹), the situation gradually changes when the operating temperature is raised, and the system becomes reversible. At 1000 °C (SOWE and solid oxide fuel cell, SOFC, operation), there is a continuous transition between water electrolysis and fuel cell current–voltage polarization curves.

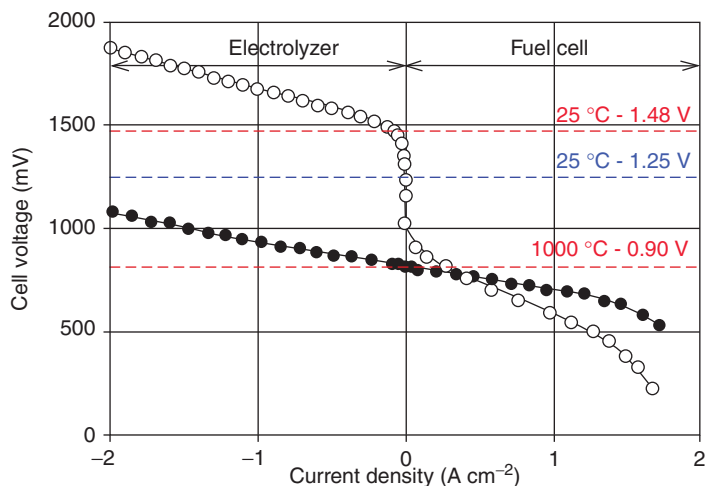


Figure 2.13 Experimental water electrolysis polarization curves measured at (○) 90 °C and (●) 1000 °C.

2.3.4

Role of Operating Pressure on the Kinetics

From the thermodynamic viewpoint, temperature and pressure play an opposite role on the electrolysis voltage. The free energy electrolysis voltage decreases by approximately $-0.8 \text{ mV } ^\circ\text{C}^{-1}$ and increases by about $+0.3 \text{ mV bar}^{-1}$. From the

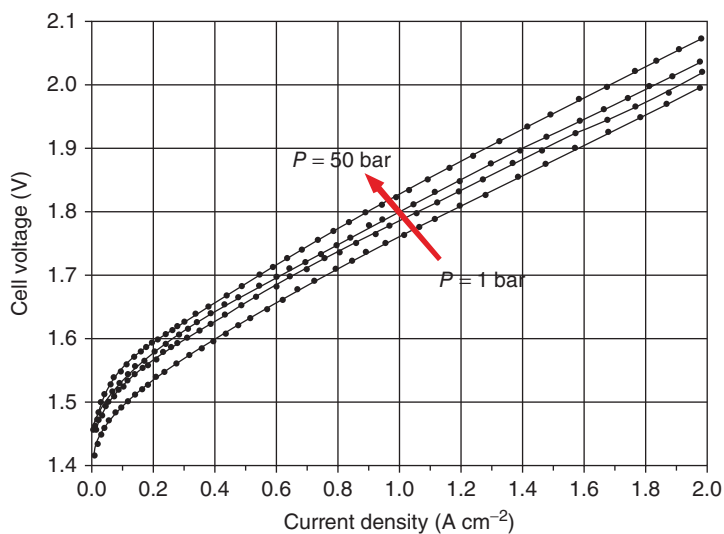


Figure 2.14 Role of operating pressure on the polarization curves of a PEM water electrolysis cell using platinum as the cathodic catalyst and iridium as the anodic catalyst.

kinetic viewpoint, a higher operating pressure usually has limited impact on the kinetics, even at the cathode where the reaction is highly reversible. In some cases (depending on the cell design and the porosity of the current collectors), a higher operating pressure can have positive effects by facilitating transport of gas bubbles. More recent and more accurate measurements show that the effect is limited, at least over the 1–50 bar range (Figure 2.14). It can be concluded that pressurized water electrolysis does not add significant energy costs compared to atmospheric water electrolysis, either in alkaline [25] or in acidic [26, 27] media, thus offering some interesting opportunities for direct storage of compressed gases as long as the capex is not too negatively penalized.

2.4

Conclusions

As discussed in the previous sections, water electrolysis can take place over an extended range of operating temperatures (from room temperature up to 800 °C) and using electrolytes of different pH. Different technologies, each of them having specific advantages and drawbacks, have been developed for operation in these different conditions. At low temperature ($T < 150$ °C), the alkaline technology based on zero-gap cell and liquid electrolyte is the more mature process. The acidic PEM technology based on the concept of a polymer electrolyte cell is more recent and increasingly considered as the water electrolysis technology of the near future. At the same time, as R&D is making progress, different materials (electrolytes and electrocatalysts) have become available. Polymers capable of operation at higher temperature (up to 250–300 °C) are becoming available. Oxide-ion-conducting materials operating down to the less aggressive 650 °C range are appearing and proton-conducting ceramics for operation in the intermediate temperature range are being studied extensively. More details are provided in the next chapters.

Nomenclature

A	membrane area (m^2)
a_i	activity of species i
C_i	concentration of species i in $\text{mol}\cdot\text{m}^{-3}$
D_i	diffusion coefficient of species i ($\text{m}^2\cdot\text{s}^{-1}$)
E	free energy electrolysis voltage (V)
F	Faraday constant ($96\,485$ °C·mol $^{-1}$)
f_i	fugacity of species i
G	Gibbs free energy ($\text{J}\cdot\text{mol}^{-1}$)
H	enthalpy ($\text{J}\cdot\text{mol}^{-1}$)
I	current (A)
i	current density (A cm^{-2})
i_0	exchange current density (A cm^{-2})

m	mole number
n	number of electrons exchanged during the electrochemical reaction
P	pressure (Pa)
p_i	partial pressure of component i in a gas mixture (Pa)
R	resistance (Ω)
r	specific resistance ($\Omega \cdot \text{m}^2$)
R_{PG}	constant of perfect gas ($0.082 \text{ J} \cdot \text{K}^{-1} \cdot \text{mol}^{-1}$)
S	entropy ($\text{J} \cdot \text{mol}^{-1} \cdot \text{K}^{-1}$)
t	time (s)
T	absolute temperature (K)
U_{cell}	cell voltage (V)
V	thermo-neutral electrolysis voltage (V)
\bar{V}	molar volume ($\text{m}^3 \cdot \text{mol}^{-1}$)
W	electrical work (J)
x, y, z	space coordinates

Greek symbols

δ	membrane thickness (m)
Δ	difference
ε	cell efficiency (%)
η	overvoltage (V)
φ	electrode absolute potential (V)
ρ	electrical resistivity ($\Omega \text{ m}$)
σ	electrical conductivity (S m^{-1})

Subscripts or superscripts

0	standard conditions (298 K, 1 bar)
cell	electrolysis cell
d	dissociation
e	electrolyte
i	species i
r	real
t	theoretical

Acronyms

MEA	membrane-electrode assembly
PEM	polymer electrolyte membrane
PGM	platinum group metals
SPE	solid polymer electrolyte
SOFC	solid oxide fuel cells
SOWE	solid oxide water electrolysis

References

- Liu, R.S. Sun, X Liu, H. Zhang, L. and Zhang, J. (2011) 'Electrochemical Technologies for Energy Storage and Conversion', *chapter 9, Water electrolysis for hydrogen generation*, (ed. J. Wiley&Sons).
- Meyer, C.A. (1993) *ASME Steam Tables: Thermodynamic and Transport Properties of Steam*, American Society of Mechanical Engineers, New York.
- LeRoy, R.L., Bowen, C.T., and Leroy, D.J. (1980) The thermodynamics of aqueous water electrolysis. *J. Electrochem. Soc.*, **127**, 1954.
- Mauritz, K.A. and Moore, R.B. (2004) State of understanding of nafion. *Chem. Rev.*, **104**, 4535–4585.
- Onda, K., Kyakuno, T., Hattori, K., and Ito, K. (2004) Prediction of production power for high-pressure hydrogen by high-pressure water electrolysis. *J. Power Sources*, **132**, 64–70.
- Divisek, J. and Murgin, J. (1983) Diaphragms for alkaline water electrolysis and method for production of the same as well as utilization thereof. US Patent 4,394,244.
- Vandenborre, H., Leysen, R., Nackaerts, H., Van der Eecken, D., Van Asbroeck, P., Smets, W., and Piepers, J. (1985) Advanced alkaline water electrolysis using inorganic membrane electrolyte (I.M.E.) technology. *Int. J. Hydrogen Energy*, **10** (11), 719–726.
- Hamann, C.H., Hamnett, A., and Vielstich, W. (1998) *Electrochemistry*, Wiley-VCH Verlag GmbH, Weinheim.
- Bockris, J.O.'M. and Reddy, A.A.K. (1982) *Comprehensive Treatise of Electrochemistry*, Plenum Press E.
- Grigoriev, S.A., Mamat, M.S., Dzhus, K.A., Walker, G.S., and Millet, P. (2011) Platinum and palladium nano-particles supported by graphitic nano-fibers as catalyst for PEM water electrolysis. *Int. J. Hydrogen Energy*, **36**, 4143.
- Frumkin, A.N. (1963) in *Advances in Electrochemistry and Electro-Chemical Engineering*, vol. 3 (ed. P. Delahay), Interscience, New York.
- Bockris, J.O.'M., McBreen, J., and Nanis, L. (1965) The hydrogen evolution kinetics and hydrogen entry into a-iron. *J. Electrochem. Soc.*, **112**, 1025.
- Millet, P., Durand, R., and Pineri, M. (1989) New solid polymer electrolyte composites for water electrolysis. *J. Appl. Electrochem.*, **19**, 162–166.
- Marshall, A., Børresen, B., Hagen, G., Tsytkin, M., and Tunold, R. (2009) Hydrogen production by advanced proton exchange membrane (PEM) water electrolyzers-reduced energy consumption by improved electrocatalysis. *Int. J. Hydrogen Energy*, **34**, 4974–4982.
- Bockris, J.O.'M. (1956) Kinetics theory of adsorption intermediates in electrochemical catalysis. *J. Chem. Phys.*, **24**, 817.
- Millet, P., Durand, R., and Pinéri, M. (1990) Preparation of new solid polymer electrolyte composites for water electrolysis. *Int. J. Hydrogen Energy*, **15**, 245.
- Damjanovic, A., Dey, A., and Bockris, J.O.'M. (1966) Electrode kinetics of oxygen evolution and dissolution on Rh, Ir and Pt-Rh alloy electrodes. *J. Electrochem. Soc.*, **113**, 739.
- Krasil'shchikov, A.I. (1963) *Zh. Fiz. Khim.*, **37**, 273.
- Boodts, J.F.C., Alves, V.A., Da Silva, L.A., and Trasatti, S. (1994) Kinetics and mechanism of oxygen evolution on IrO₂ – based electrodes containing Ti and Ce acidic solutions. *Electrochim. Acta*, **39**, 1585.
- Trasatti, S. (1990) The oxygen evolution reaction, in *Electrochemical Hydrogen Technologies* (ed. H. Wendt), Elsevier, Amsterdam.
- Millet, P., Alleau, T., and Durand, R. (1993) Characterization of membrane-electrodes assemblies for Solid Polymer Electrolyte water electrolysis. *J. Appl. Electrochem.*, **23**, 322–331.
- Grigoriev, S., Ilyukhina, L.I., Middleton, P.H., Millet, P., Saetre, T.O., and Fateev, V.N. (2008) A comparative evaluation of palladium and platinum nanoparticles as catalysts in PEM electrochemical cells.

- Int. J. Nucl. Hydrogen Prod. Appl.*, **1-4**, 343–354.
23. Matsuda, A. and Ohmori, T. (1962) *J. Res. Inst. Catal., Hokkaido Univ.*, **10**, 203.
 24. Pierozynski, B. (2011) On the hydrogen evolution reaction at nickel-coated carbon fibre in 30 wt. % KOH solution. *Int. J. Electrochem. Sci.*, **6**, 63–77.
 25. Schug, C.A. (1998) Operational characteristics of high pressure, high efficiency, water-hydrogen electrolysis. *Int. J. Hydrogen Energy*, **23**, 1113–1120.
 26. Engel, R.A., Chapman, G.S., Chamberlin, C.E., and Lehman, P.A. (2004) Development of a high pressure PEM electrolyzer: enabling seasonal storage of renewable energy. Proceeding of the 15th Annual U.S. Hydrogen Conference, Los Angeles, CA, April 26–30, 2004.
 27. Marangio, F., Pagani, M., Santarelli, M., and Cali, M. (2011) Concept of a high pressure PEM electrolyser prototype. *Int. J. Hydrogen Energy*, **36**, 7807–7815.